



Article

Construction of a High-Density Genetic Linkage Map Based on Bin Markers and Mapping of QTLs Associated with Fruit Size in Jujube (*Ziziphus jujuba* Mill.)

Tianfa Guo ^{1,2,†}, Qianqian Qiu ^{1,2,†}, Fenfen Yan ^{1,2}, Zhongtang Wang ³, Jingkai Bao ^{1,2}, Zhi Yang ^{1,2}, Yilei Xia ^{1,2}, Jiurui Wang ⁴, Cuiyun Wu ^{1,2,*} and Mengjun Liu ^{1,2,5,*}

- ¹ The National and Local Joint Engineering Laboratory of High Efficiency and Superior-Quality Cultivation and Fruit Deep Processing Technology of Characteristic Fruit Trees in Southern Xinjiang, Aral 843300, China; gtfzky@taru.edu.cn (T.G.); zkyqqq1025@126.com (Q.Q.); yanfening@163.com (F.Y.); baomouren1997@163.com (J.B.); yangzhi950103@outlook.com (Z.Y.); xyl128@126.com (Y.X.)
- ² College of Horticulture and Forestry, Tarim University, Aral 843300, China
- ³ Shandong Institute of Pomology, Tai'an 271000, China; sdgss213@163.com
- ⁴ College of Forestry, Hebei Agricultural University, Baoding 071000, China; wjrjujube@126.com
- ⁵ College of Horticulture, Hebei Agricultural University, Baoding 071000, China
- * Correspondence: wcyby@taru.edu.cn (C.W.); lmj1234567@aliyun.com (M.L.); Tel.: +86-136-575-68050 (C.W.); +86-139-322-62298 (M.L.)
- † These authors contributed equally to this work.

Abstract: Jujube (*Ziziphus jujuba* Mill.) is a fruit tree that is gaining increasing importance in drought-affected regions worldwide. The fruit size is an important quantitative agronomic trait that affects not only the fruit yield and attractiveness but also consumer preference. Genetic enhancement of fruit appearance is a fundamental goal of jujube breeding programs. The genetic control of jujube fruit size traits is highly quantitative, and development of high-density genetic maps can facilitate fine mapping of quantitative trait loci (QTLs) and gene identification. However, studies regarding the construction of high-density molecular linkage maps and identification of quantitative trait loci (QTLs) targeting fruit size in jujube are limited. In this study, we performed whole-genome resequencing of the jujube cultivars “JMS2” and “Xing16” and their 165 F_1 progenies to identify genome-wide single-nucleotide polymorphism (SNP) markers and constructed a high-density bin map of jujube that can be used to assist in the selection of multiple traits in jujube breeding. This analysis yielded a total of 116,312 SNPs and a genetic bin map of 2398 bin markers spanning 1074.33 cM with an average adjacent interval of 0.45 cM. A quantitative genetic analysis identified 15 QTLs related to fruit size and the observed phenotypic variation associated with a single QTL ranged from 9.5 to 13.3%. Through the screening of overlapping and stable QTL regions, we identified 113 candidate genes related to fruit size. These genes were ascertained to be involved in cell division, cell wall metabolism, synthesis of phytohormones (ABA, IAA, and auxin), and encoding of enzymes and transcription factors. These candidate genomic regions will facilitate marker-assisted breeding of fruits with different sizes and shapes and lay a foundation for future breeding and manipulation of fruit size and shape in jujube.

Keywords: jujube; whole-genome resequencing; bin map; QTL; fruit size



Citation: Guo, T.; Qiu, Q.; Yan, F.; Wang, Z.; Bao, J.; Yang, Z.; Xia, Y.; Wang, J.; Wu, C.; Liu, M. Construction of a High-Density Genetic Linkage Map Based on Bin Markers and Mapping of QTLs Associated with Fruit Size in Jujube (*Ziziphus jujuba* Mill.). *Horticulturae* **2023**, *9*, 836. <https://doi.org/10.3390/horticulturae9070836>

Academic Editor: Yuepeng Han

Received: 5 May 2023

Revised: 9 June 2023

Accepted: 12 June 2023

Published: 22 July 2023



Copyright: © 2023 by the authors. Licensee MDPI, Basel, Switzerland. This article is an open access article distributed under the terms and conditions of the Creative Commons Attribution (CC BY) license (<https://creativecommons.org/licenses/by/4.0/>).

1. Introduction

Chinese jujube (*Ziziphus jujuba* Mill., $2n = 2x = 24$) belongs to the genus *Ziziphus* and is one of the most economically important members of the Rhamnaceae family [1–4]. Native to China, it is one of the oldest cultivated fruit trees in the world with over 7000 years of cultivation history and is now a major dry fruit crop [5]. At present, more than 90% of jujube production is concentrated in six provinces: Xinjiang, Hebei, Shandong, Shanxi, Shaanxi, and Henan. It is the foremost dry fruit in terms of production and the main income source of ~20 million farmers in China [2,3]. It is well adapted to various biotic

and abiotic stresses, especially drought and salinity, and is considered an ideal cash crop for arid regions, such as Xinjiang. Although jujube cultivation is several thousand years old [5,6], jujube fruit quality traits, such as the size and flesh flavor, still require significant improvement to satisfy consumer preference. Understanding the molecular mechanism of genes controlling fruit quality is the key to developing jujube cultivars with improved fruit quality.

Highly saturated genetic linkage maps are essential for the fine localization of genes, marker-assisted selection (MAS), and structural and functional genomics. Marker-assisted quantitative trait locus (QTL) studies have used genetic linkage maps to dissect the genetic basis of complex traits in several horticulture plants [7–9]. The first genetic map of jujube, developed from 72 progeny of the cultivars “Dongzao” and “linyilizao”, was constructed using random amplified polymorphic DNA (RAPD) makers [10]. In this case, the use of RAPD markers led to a separate map for each of the parents, which had unequal number of linkage groups. Due to the lack of genomic information, the number of available markers in the map was small and the repeatability was poor. The inability to distinguish between homo- and heterozygosity meant this method was unable to capture complete genetic information in jujube. Later studies used codominant AFLP and SSR markers for genetic map construction [11–13], but the resulting map density was too limited for fine mapping of traits of interest in jujube.

With the availability of draft jujube genome assemblies and genome resequencing data based on next-generation sequencing platforms [14], a genetic linkage map of jujube with the most comprehensive genome coverage, the largest number of markers, and the largest marker density has been constructed [15,16]. The markers can improve genetic resolution to fine map qualitative traits and facilitate map-based gene cloning in jujube [17]. However, the tools and approaches required to develop genetic maps from millions of markers from genome resequencing projects are not available, and some data reduction approaches are useful to obtain the most informative markers for further analysis [18].

Bin markers are continuous SNPs occurring at nonrecombining intervals in the genome. They have the advantages of being computationally less intensive and highly accurate, having better density, and being more precisely mapped and cost-effective [19]. In combination with whole-genome sequencing approaches, the bin mapping strategy helps to construct highly dense genome-wide linkage maps by capturing rare recombination events in segregating populations. For example, Peng et al. used a multiomics approach that integrated whole-genome resequencing-based quantitative trait locus (QTL) mapping with an F_1 population, population genomics analysis using germplasm accessions, and transcriptome analysis to identify genomic regions that are potentially associated with fruit weight in loquat [20]. Therefore, the bin mapping approach is highly suited to reducing the sequencing datasets by keeping the most informative markers for high-density genetic map construction and QTL identification [18].

Fruit size is an integral part of fruit quality and directly influences the commodity value and economic return of fruit crops. Linkage-map-based identification of molecular markers or genes of interest and molecular-marker-assisted breeding hold enormous promise. Thus, their application is urgently needed to improve the existing cultivars of jujube. Despite the importance of fruit size, its underlying molecular mechanisms remain understudied in jujube. Studies have shown that fruit size traits are controlled by polygenes with weak inheritability [21] and are directly or indirectly regulated by one or more hormones [22,23].

In this study, we report a high-density bin-marker-based genetic map on fruit size in Chinese jujube. The stably inherited major QTLs were screened, and the candidate genes determining fruit size were mined. The results obtained lay a foundation for employing MAS in breeding programs, fine mapping, and cloning of crucial genes in jujube.

2. Materials and Methods

2.1. Test Materials and Phenotypic Determination

Because it is difficult to construct F_2 populations in fruit trees, F_1 generation is generally used as the material for constructing genetic maps. For example, in apples [24], pears [18,25], grapes [26], and apricots [27], F_1 hybrids have been used as materials for mapping. In this study, an F_1 segregating population consisting of 165 progenies obtained from a “JMS2” × “Xing16” cross conducted by Prof. Liu Mengjun and team at the Hebei Agricultural University, Hebei, China, was used. They were planted with a spacing of 1 × 3 m in a jujube orchard (80°28′ E, 40°59′ N) located in Aral City, China, in 2018. In 2019, 2020, and 2021, 30 representative fruits with uniform size, no pests and diseases, and normal development at the fully red mature stage were picked from each progeny and each of their two parents as representative samples. SFW, FLD, and FTD were measured according to the method described in the Germplasm Resources of Chinese Jujube [6].

2.2. Extraction of Genomic DNA, Library Construction, and Sequencing

In mid-May 2020, the healthy young leaves of each progeny and the two parents were harvested, cleaned, placed into numbered cryovials, flash-frozen in liquid N, and stored in a −80 °C ultralow temperature laboratory freezer. Total genomic DNA was extracted by the CTAB method and randomly digested into 150 bp long fragments [28]. The library construction involved end repair, the addition of polyA to the 3′ end, ligation of sequencing adapters, purification, and PCR-based amplification. After stringent quality checks, the libraries were paired end to end and sequenced using an HiSeq™2500 platform (Illumina, San Diego, CA, USA).

2.3. SNP Marker Screening and Genotyping

The raw reads were filtered to obtain clean reads by eliminating the adapters, reads with >10% of bases, and reads of low quality [29]. The cleaned reads were aligned to the jujube reference genome of “Dongzao” [14] using the Burrows–Wheeler Aligner (BWA) software [30]. The read pairing information and flags on the BWA (sequence alignment/map format) records were first cleaned up using the Duplicates tool (Picard: <http://sourceforgr.net/projects/picard/> (accessed on 18 September 2020)) to shield the effect of PCR duplication. InDel realignment was performed using GATK [31], that is, the sites near the insertion–deletion alignment results were partially realigned to correct the alignment error caused by the insertion–deletion. Base recalibration was performed using GATK to correct the base mass value. GATK was used for variant calling, including SNP and InDel [32]. Based on the minimum recombination fragment identified in each progeny, the SNP segments that did not undergo recombination in each progeny were combined, thus forming a bin marker. All of the sequences of the bin markers that were used to construct the linkage map were aligned to the physical sequences of the reference genome. In order to ensure the quality of the bin mapping, the genotype homozygosity; parental marker depths of 1×, 2×, and 3×; and markers located on nonchromosomal markers were not considered. High-depth sequencing parents were used to fill in relatively correct genotypes and correct the genotypes of low-depth offspring to ensure the correctness of offspring typing.

2.4. Construction of Genetic Linkage Map

In order to ensure the quality of the map, the markers were filtered and screened using the following methods: (1) remove markers with homozygous parents; (2) ensure parental marker depth is not less than 4×; (3) remove nonchromosomal markers. According to the parental genotyping of the offspring, high-depth parental sequencing ensures the correctness of offspring typing. The linkage group was divided by the chromosome of the marker, and the genetic linkage test was performed on the two markers. The linkage phase was determined according to the recombination rate of markers. Wrong genotypes were corrected using genotypes with relatively definite linkage. After marker filling and

correction, the bin was divided according to the recombination of offspring. The samples were arranged neatly according to the physical position of the chromosome. When there was a typing change in any sample, it was considered that there was a recombination breakpoint. The SNP between the recombination breakpoints was classified as bin, and there was no recombination time in bin. Finally, the genetic map was constructed using the bin as a mapping marker. The bin was divided into 15 linkage groups based on known information. The linear arrangement of markers in the linkage group was analyzed by HighMap (<http://highmap.biomarker.com.cn> (accessed on 24 February 2021)) [33] software, and the genetic distance between adjacent markers was estimated.

2.5. Gene Mapping and Nomenclature of QTLs

The CIM method in R/QTL [34] was used to locate the QTLs related to SFW, FLD, and FTD in the F_1 population, and those with an LOD ≥ 3 were considered to be effective in determining fruit size [35,36]. The QTL determining a specific phenotypic trait was named using the following pattern: abbreviation of the English name of the trait + year + the number of the LG it is mapped to + the code number of QTL, e.g., FW19.1.1 indicates that the trait of SFW identified in 2019 was located in LG1 and belonged to QTL1. If the same trait overlapped in the same location repeatedly over a period of two or more years and demonstrated an LOD ≥ 3.0 and a PVE $\geq 10\%$, the QTL identified at that location was considered to exist stably. Thus, the genes in these stable QTLs had a higher probability of regulating the fruit size and could be screened to serve as candidate genes for this trait.

2.6. Screening and Annotation of Candidate Genes

The markers within the acceptable confidence interval associated with the stable QTLs described in the previous section were compared with the genome of “Dongzao” as a reference [GCF_000826755.1_ZizJuj_1.1] (https://www.ncbi.nlm.nih.gov/genome/15586?genome_assembly_id=219393 (accessed on 1 February 2021)). Functional annotation and alignment were performed using the relevant sequences obtained from the COG, GO, KEGG, Swissprot, and Nr5 databases. Based on the screening results of the functional annotation studies, the candidate genes not related to the trait of fruit size were excluded but those related to fruit size were identified as putative genes.

2.7. Data Processing and Analysis

The software OriginPro 8.5 (OriginLab, Northampton, MA, USA) was used to draw the frequency distribution histogram of the SFW, FLD, and FTD parameters. SPSS 17.0 (IBM, San Jose, CA, USA) was used to determine if the parameters of fruit size conformed to a pattern of normal distribution. The genetic transmission ability (Ta) of the parents was calculated using the following formula: $Ta = \frac{\text{the average value of the trait in the hybrid offspring}}{\text{the average value of the trait in both the parents}} \times 100\%$.

3. Results

3.1. Identification of SNP Markers Based on Whole-Genome Resequencing Data

A total of 386.5 GB of filtered data were obtained through the whole-genome resequencing (WGRS) of the female parent “JMS2,” the male parent “Xing16,” and their 165 progenies, with 13.93, 9.92, and 362.65 GB of individual data, respectively, with an average Q30 and GC content of 93.21 and 33.80% (Table 1). The sequencing reads of all three groups demonstrated an alignment rate of $>90\%$ and average coverage depths of $28\times$, $19\times$, and $4.14\times$, respectively, compared to the genome of the jujube cultivar “Dongzao” used as a reference [14]. The genome coverage was $>80\%$ (covering at least $1\times$) for the two parents and 76.33% (covering at least $1\times$) for the progeny. The results obtained indicated that the sequenced DNA samples had a low error rate.

Table 1. Resequencing data statistics of “JMS2” × “Xing16” F_1 segregating population.

Sample	Total Clean Bases (Gb)	Q30 Proportion (%)	GC Proportion (%)	Average Sequencing Depth (×)	Mapped (%)	Coverage Ratio (%)
Female parent	13.93	93.19	33.71	28×	97.91	87.31
Male parent	9.92	93.61	33.74	19×	97.84	86.24
Offspring	362.65	92.82	33.96	4.14×	97.04	76.33

A total of 1,569,033 SNPs were detected through a comparative study between the genomes of the parents with a transition/transversion ratio (Ti/Tv) of 1.75 (Table 2). The number of heterozygous and homozygous SNPs in “JMS2” were 615,822 and 953,211, respectively, while those in “Xing16” were 713,815 and 855,218, respectively. A total of 148,738 SNPs with a depth not less than 4× were found suitable for coupling (CP). The parents and their progeny were rigorously screened and filtered for the four genotype-specific markers “nn × np” (n = 41,094), “Im × II” (n = 51,657), “hk × hk” (n = 23,405), and “ef × eg” (n = 156), which accounted for 78.2% of the total number of markers identified. Finally, 116,312 SNPs were retained for constructing bin markers using filtered data by referring to a previously described method [37].

Table 2. Statistics of SNPs obtained from “JMS2” and “Xing16” detection.

Parents	SNP Number	Transition Number	Transversion Number	Ti/Tv Ratio	Heterozygous SNP Number	Homozygous SNP Number
Female parent	1,569,033	998,634	570,399	1.75	615,822	953,211
Male parent	1,569,033	998,634	570,399	1.75	713,815	855,218

3.2. Construction of a High-Density Genetic Map Using the F_1 Segregating Population Obtained from “JMS2” × “Xing16”

Based on the genomic sequence of the jujube cultivar “Dongzao” as a reference (https://www.ncbi.nlm.nih.gov/genome/15586?genome_assembly_id=219393 (accessed on 24 February 2021)), the 116,312 SNPs were combined to form 2398 bin markers (each containing an average of 49 SNP markers) using consecutive SNPs derived from all offspring of the same parent. These bin markers were then used for the molecular mapping of selected genes. A genetic map was constructed with a total map distance of 1074.33 cM containing 12 LGs and an average distance of 0.45 cM between adjacent markers. The 12 LGs ranged in length from 67.43 (LG9) to 124.86 (LG6) cM, the number of bin markers ranged from 135 (LG9) to 263 (LG1) cM, and the average intertag distance ranged from 0.38 (LG1) to 0.52 (LG3) cM. The largest intertag distance was 7.76 cM (LG1), followed by LG2, 3, and 9 (7.06 cM in all). The probability of gaps < 5 cM in length in the 12 LGs ranged from 99.25 to 100%, and the average length of 99.61% of the gaps between consecutive markers was < 5 cM. LG6 and 9 were the longest and shortest LGs, respectively (Figure 1), and the largest gap of 82–90 cM was in LG1 (Table 3).

Table 3. Distribution of bin markers on the high-density genetic map constructed.

Linkage Group	Number of Bin Markers	Number of SNP Markers	Genetic Length (cM)	Average Distance (cM)	Max Gap (cM)	Gap < 5 cM (%)
LG1	263	16,203	99.45	0.38	7.76	99.62
LG2	211	10,638	96.26	0.46	7.06	99.52
LG3	188	9802	98.36	0.52	7.06	99.47
LG4	228	10,716	92.54	0.41	4.05	100.00
LG5	182	11,390	77.14	0.42	2.46	100.00

Table 3. Cont.

Linkage Group	Number of Bin Markers	Number of SNP Markers	Genetic Length (cM)	Average Distance (cM)	Max Gap (cM)	Gap < 5 cM (%)
LG6	249	9032	124.86	0.50	5.37	99.60
LG7	165	9878	67.46	0.41	1.83	100.00
LG8	221	8205	96.89	0.44	5.70	99.55
LG9	135	9366	67.43	0.50	7.06	99.25
LG10	206	7228	99.12	0.48	6.38	99.51
LG11	151	6948	71.71	0.47	5.04	99.33
LG12	199	6906	83.11	0.42	5.04	99.49
Totals	2398	116,312	1074.33	-	-	-
Overall average	-	-	-	0.45	-	99.61
Max	-	-	-	-	7.76	-

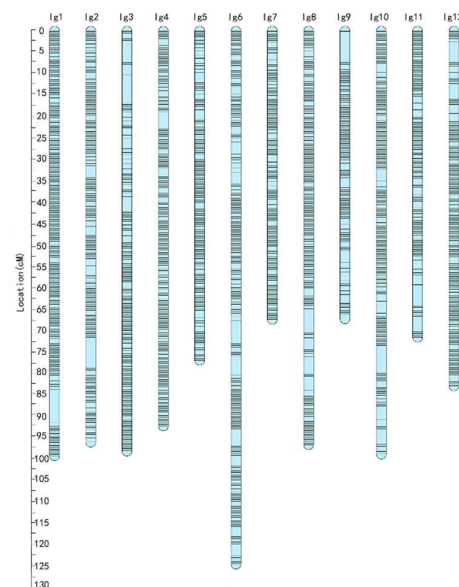


Figure 1. The high-density genetic linkage map. Distribution of bin markers on 12 LGs. A black bar indicates a bin marker. The LG number is shown on the *x*-axis, and the genetic distance in cM is shown on the *y*-axis.

3.3. Phenotypic Analysis of Traits Relating to Fruit Size in the F_1 Segregating Population

The values of the three indicators of fruit size in the two parents “JMS2” and “Xing16” and the F_1 segregating population derived from them were determined over a period of three years: 2019, 2020, and 2021 (Table 4). The average values of fruit size in “JMS2” were significantly higher than those in “Xing16” in all three years. The transmission of parental genetic information showed the following pattern with regard to importance: FTD > FLD > SFW. The absolute values of skewness and kurtosis in the F_1 population were <2, which conformed to a pattern of continuous normal distribution. The results obtained were consistent with the number distribution plot, showing that the three typical quantitative trait characteristics selected were suitable for use in QTL mapping (Figure 2). In addition, three years of phenotypic data showed a significant positive correlation between SFW, FLD, and FTD, indicating that the single fruit weight and the vertical and horizontal diameter can influence each other (Table 5).

Table 4. Statistics of fruit size traits in two parents and their F_1 population over three years.

Traits	Year	Parents			F_1 population			
		JMS2	Xing16	Range	Mean \pm SD	Ta %	Skewness	Kurtosis
Single fruit weight (g)	2019	11.00	2.76	1.02–8.45	4.30 \pm 1.38	62.52	0.200	0.287
	2020	10.50	2.81	1.46–13.41	5.47 \pm 1.99	82.22	0.989	1.817
	2021	7.82	2.52	1.67–9.01	4.45 \pm 1.38	86.09	0.574	0.557
Fruit longitudinal diameter (mm)	2019	34.47	17.76	15.04–27.19	20.87 \pm 2.64	79.92	0.020	−0.509
	2020	35.04	18.49	14.32–32.49	22.33 \pm 3.18	83.44	0.200	0.108
	2021	32.58	17.45	14.88–31.34	21.40 \pm 2.71	85.54	0.566	1.205
Fruit transverse diameter (mm)	2019	25.58	16.16	12.27–23.57	19.22 \pm 2.44	92.10	−0.512	0.111
	2020	24.88	16.56	13.60–28.20	20.83 \pm 2.74	100.53	0.146	0.067
	2021	21.70	16.44	13.71–24.49	19.27 \pm 2.24	101.04	0.566	1.205

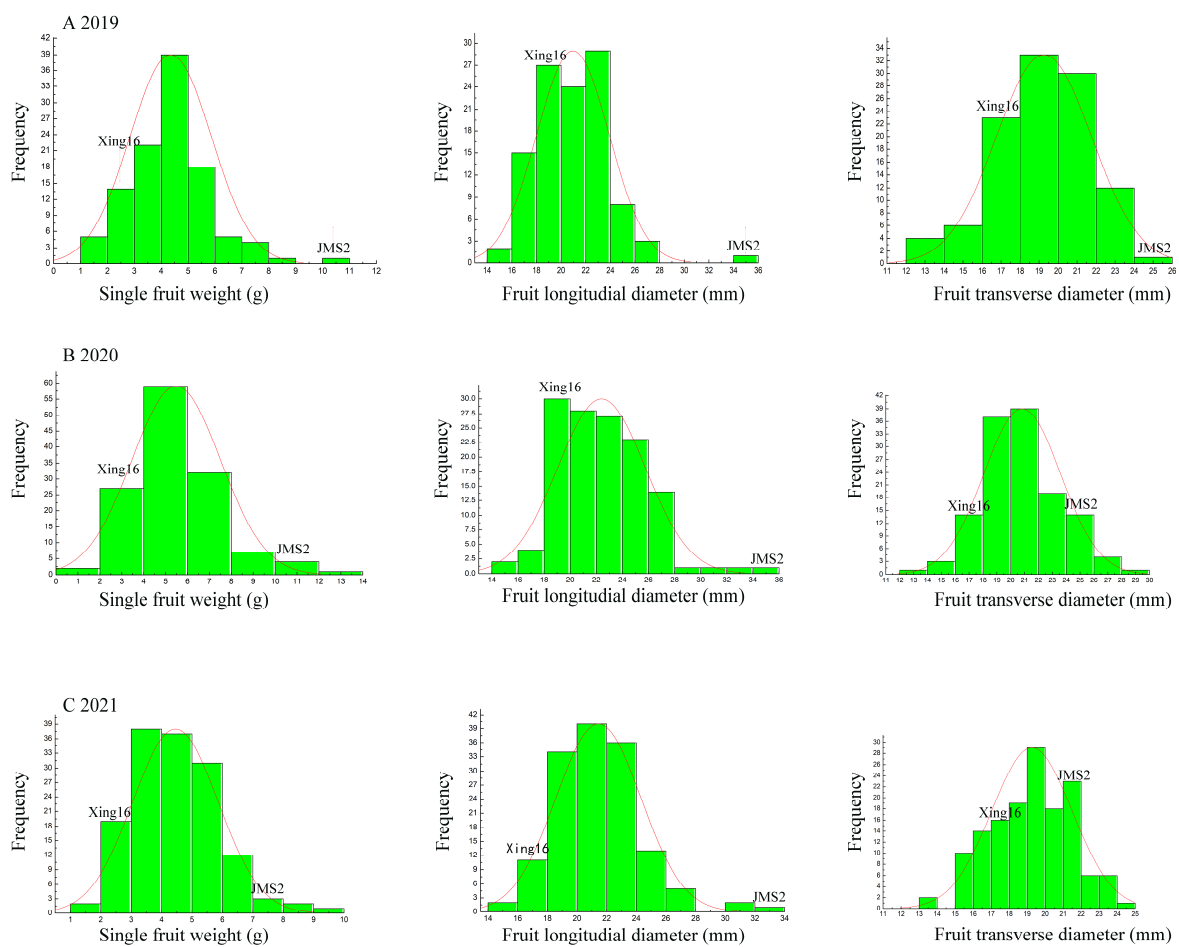


Figure 2. Frequency distribution of fruit size traits in the parents and the F_1 population over a three-year duration. Frequency distributions of SFW, FLD, and FTD in progenies of the “JMS2” and “Xing16” hybrid cross. The phenotypic data were collected in (A) 2019, (B) 2020, and (C) 2021. The vertical coordinates correspond to the columns in which “JMS2” and “Xing16” are located in the figure and indicate the range of the phenotypic values of SFW, FLD, and FTD in the parents. The horizontal coordinates indicate the number of progenies occurring within the range of phenotypic values.

Table 5. Correlation analysis of traits relating to fruit size in the F_1 segregating population.

Year	FW vs. FLD	FW vs. FTD	FLD vs. FTD
2019	0.8360 **	0.9280 **	0.7512 **
2020	0.8771 **	0.9424 **	0.7972 **
2021	0.8291 **	0.9370 **	0.6832 **

Double asterisks (**) indicated extremely significant correlation at $p < 0.01$ level; SFW stands for Single fruit weight; FLD stands for Fruit longitudinal diameter; FTD stands for Fruit transverse diameter.

3.4. QTL Analysis of Traits Relating to Fruit Size in the F_1 Segregating Population Derived from “JMS2” × “Xing16”

Based on the high-density bin marker map described in the previous section and the phenotypic data for SFW, FLD, and FTD obtained over three years, a total of 19 QTLs associated with these three fruit size traits were mapped to seven chromosomes/LGs with a phenotypic interpretation range of 9.5–13.3% (Table 6). The number of QTLs detected on LG2, 4, 6, 7, 8, 11, and 12 was 7, 1, 3, 1, 2, 3, and 2, respectively. In 2019 and 2020, QTL FTD2.1 was repeatedly detected on LG2. Its yearly phenotypic interpretation rates were 13.3 and 10.5% and its annual LOD thresholds were 3.08 and 3.35, respectively, due to which it was recognized as the most effective QTL in determining fruit size. All the other QTLs could only be detected in 2019 or 2020. However, the LOD thresholds of FW21.2.2, FLD21.2.1, and FTD21.8.1 were all >3.5 and their contribution rates were $>10\%$, due to which they too were regarded to be equally effective QTLs.

Table 6. QTL mapping of traits relating to fruit size in the F_1 segregation population.

Trait	QTLs	Intervals on Maps (cM)	LOD	Peak Marker Position (cM)	PVE (%)	Containing Markers
Single fruit weight	FW20.11.1	20.475–21.382	3.15	20.475	10.7	2
	FW21.2.1	91.738–92.944	3.44	92.644	10.8	3
	FW21.2.2	94.45–96.259	3.63	94.45	11.3	4
	FW21.12.1	28.383	3.02	28.383	9.5	1
	FTD19.2.1	91.437–91.738	3.08	91.437	13.3	2
	FTD20.4.1	18.968–23.921	3.27	23.02	11.1	5
	FTD20.6.1	111.226	3.02	111.226	10.3	1
	FTD20.6.2	113.029–113.93	3.15	113.33	10.7	4
Fruit transverse diameter	FTD20.6.3	122.75	3.2	122.75	10.9	1
	FTD20.11.1	21.382	3.04	21.382	10.3	1
	FTD20.11.2	47.29–47.891	3.04	47.891	10.4	3
	FTD21.2.1	91.738–92.944	3.35	92.644	10.5	3
	FTD21.2.2	94.45	3.07	94.45	9.7	1
	FTD21.2.3	95.352–96.259	3.15	95.352	9.9	2
	FTD21.8.1	64.38–86.663	4.51	71.891	13.9	18
	FTD21.8.2	92.085	3.00	92.085	9.5	1
Fruit longitudinal diameter	FTD21.12.1	27.783–28.683	3.47	28.383	10.9	4
	FLD21.2.1	91.137–96.259	3.91	94.45	12.1	11
	FLD21.7.1	38.567–39.468	3.10	38.867	9.7	4

The QTLs were, however, not evenly distributed among all the LGs/chromosomes. Certain LGs contained QTLs influencing multiple indicators of fruit size, with some even clustered in the same regions (Figure 3). There was an overlap between FTD21.1, FW21.1, and FLD21.1 on LG2 with a length of 91.738–92.944 cM, which was linked to all three traits SFW, FLD, and FTD simultaneously. Another overlap zone between FW21.2, FTD21.2, and FLD21.1 was found on LG2 with a length of 94.45–96.259 cM. This region is associated with fruit weight and size. One overlap zone between FW21.1 and FTD21.1 with a length of 28.383 cM on LG12 and another one between FW20.1 and FTD20.1 with a length of 21.382 cM on LG11 were identified with SFW and FTD, respectively. These genetic regions

identified with QTLs demonstrating stable effects are worthy of attention in follow-up studies (Table 7).

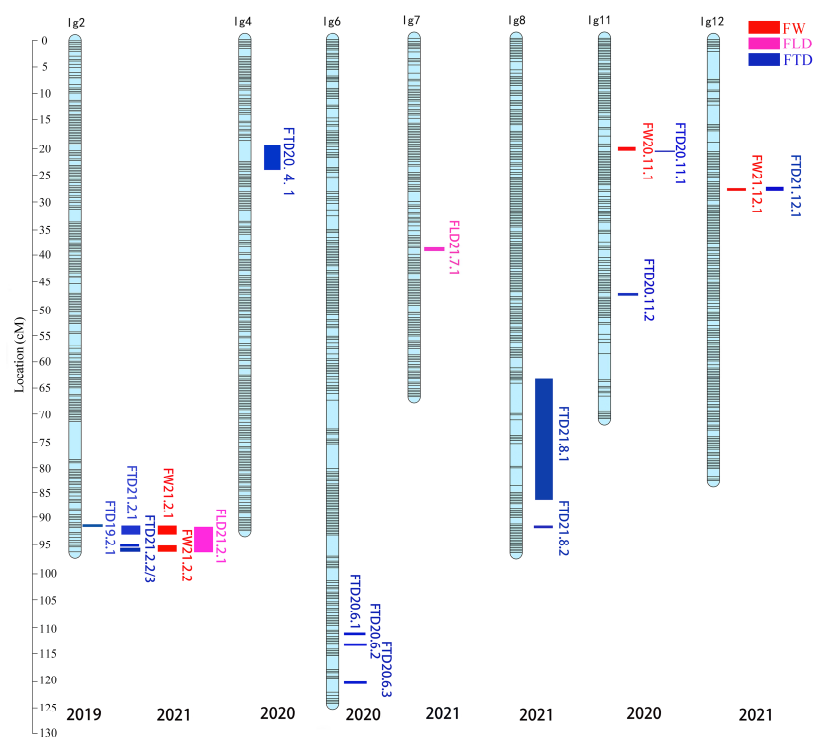


Figure 3. The QTLs distribution map of fruit size-related traits. The CIM method in R/qtl was used to locate the QTLs regarding SFW, FLD, and FTD in the F_1 population, and loci with $LOD \geq 3$ were considered to be effective. The QTL determining a specific phenotypic trait was named using the following pattern: abbreviation of the English name of the trait + year + the number of the LG it is mapped to + the code number of the QTL. The letters LG on the top of the linkage maps represent “linkage group”, and the number following LG indicates the number of the linkage group. The QTLs for SFW, FLD, and FTD are marked with red, pink, and blue colored bars, respectively.

Table 7. QTL cluster information of traits relating to fruit size.

Traits	Corresponding QTL	Coincidence Interval (cM)	Marker Number	LG
Fruit transverse diameter, Single fruit weight, Fruit longitudinal diameter	FTD21.1, FW21.1, FLD21.1	91.738–92.944	3	2
Single fruit weight, Fruit transverse diameter, Fruit longitudinal diameter	FW21.2, FTD21.2, FLD21.1	94.450–96.259	4	2
Fruit transverse diameter, Single fruit weight	FTD21.1, FW21.1	28.383	1	12
Fruit transverse diameter, Single fruit weight	FTD20.1, FW20.1	21.382	1	11

3.5. Prediction of the Putative Functions of Candidate Genes

The candidate genes influencing fruit size were identified based on the markers mapped within the 15 QTLs and their physical location on the “Dongzao” genome. The genes were mined from five databases, namely, Clusters of Orthologous Groups (COG, [38]), Gene Ontology (GO, <http://geneontology.org/> (accessed on 22 July 2021 and 7 July 2022)), Kyoto Encyclopedia of Genes and Genomes (KEGG, Kanehisa Laboratories, Kyoto University), Swissprot (<http://www.uniprot.org/> (accessed on 22 July 2021 and 7 July 2022)), and

Nr (NCBI), to determine the tag information, markers, and genes in the associated regions. The candidate QTLs that were identified in any two years of the study period concerning at least two of the three indicators concerning fruit size or with LOD threshold ≥ 3.5 and PVE $\geq 10\%$ in any one year were selected for gene mining. A total of 727 genes were mined (Table 8).

Table 8. Genes in the associated regions by comparing the databases.

LG	Coincidence Interval (cM)	QTL Lloci	Gene Number	COG Anno	GO Anno	KEGG Anno	Swissprot Anno	Nr Anno
2	91.738	FTD19.1	9	3	4	5	9	9
		FTD21.1	19	0	10	10	14	19
		FTD21.1	19	0	10	10	14	19
2	91.738–92.944	FW21.1	19	0	10	10	14	19
		FLD21.1	99	33	60	40	71	99
		FW21.2	61	21	36	21	47	61
2	94.450–96.259	FTD21.2	41	12	24	16	32	41
		FLD21.1	99	33	60	40	71	99
		FTD21.1	30	12	25	14	28	30
12	28.383	FW21.1	3	2	3	2	2	3
11	21.382	FTD20.1	0	0	0	0	0	0
		FW20.1	1	0	1	0	1	1
2	94.45–96.259	FW21.2	61	21	36	21	47	61
2	91.137–96.259	FLD21.1	99	33	60	40	71	99
8	64.38–86.663	FTD21.1	167	55	111	68	125	167
Total	-	-	727	225	450	297	546	727

According to the map positions of the candidate QTLs, 15 candidate genomic regions affecting traits relating to fruit size were identified, the relevant candidate genes were identified, and their functions were predicted in GO and KEGG (Table 9). Consequently, a total of 113 candidate genes possibly associated with the regulation of fruit size were identified. These genes were found to be involved in the processes of cell division, cell cycle, cell wall metabolism, and synthesis of phytohormones (ABA, IAA, and auxin) as well as encoding of enzymes, transcription factors (TFs), and zinc finger proteins (ZFPs). The genes *LOC107410242* and *LOC107409642* were related to the morphogenesis of anatomical structure and tissue development as well as regulation of gene expression and cellular and developmental processes. The genes *LOC107409953*, *LOC112490770*, *LOC107409998*, *LOC107409919*, *LOC107423923*, and *LOC107423861* were related to encoding LRR receptor-like serine/threonine protein kinases. *LOC107410143* and *LOC107423897* were associated with LRR receptor-like proteins and kinases, respectively. *LOC107410070* and *LOC107423821* were related to the cell cycle. *LOC107423912*, *LOC107423913*, *LOC107431775*, *LOC107423905*, and *LOC107423928* were related to the synthesis of phytohormones such as IAA, auxins, and cytokinins. *LOC107409704*, *LOC107423900*, *LOC107431772*, *LOC107423814*, *LOC107423857*, *LOC107423922*, *LOC107423848*, *LOC107423846*, *LOC107423858*, *LOC107423925*, *LOC107423856*, *LOC107423903*, and *LOC107423881* were related to the cell wall formation or metabolic enzyme activity. *LOC107423820* and *LOC107423815* were associated with pectin esterase. *LOC107423811* was related to the TF BHLH. *LOC107409987* was associated with a NAC domain-containing protein. *LOC107409426* was related to ZFPs. *LOC107423816*, *LOC107423801*, *LOC107423813*, and *LOC107431773* were related to E3 ubiquitin protein ligase. These genes may be involved in the regulation of fruit size in jujube.

Table 9. The genes putatively associated with jujube fruit development.

Range (cM)	QTL Name	Candidate Genes	Candidate Gene ID	Gene Annotation
	FTD19.2.1	-	-	-
91.738	FTD21.2.1	LOC107410242	rna-XM_025070976.1	anatomical structure morphogenesis;tissue development; regulation of gene expression; cellular process; developmental process; regulation of cellular process
		LOC107409642	rna-XM_016017070.2	regulation of cellular process
91.738–92.944	FW21.2.1	LOC107410242	rna-XM_025070976.1	anatomical structure morphogenesis; tissue development; regulation of gene expression; cellular process; developmental process; regulation of cellular process
		LOC107409642	rna-XM_016017070.2	regulation of cellular process
	LOC107409704	rna-XM_016017148.2	Cell wall	
	LOC107409953	rna-XM_016017375.2	LRR receptor-like serine/threonine-protein At3g47570	
	LOC112490770	rna-XM_025071274.1	LRR receptor-like serine/threonine-protein EFR	
	LOC107410143	rna-XM_016017551.2	Leucine-rich repeat-containing protein	
	LOC107410070	rna-XM_016017481.1	regulation of mitotic cell cycle	
	LOC107409704	rna-XM_016017134.2	Cell wall	
	LOC107409998	rna-XM_016017417.2	LRR receptor-like serine/threonine-protein EFR	
	LOC107410070	rna-XM_025070726.1	regulation of mitotic cell cycle	
	LOC107410070	rna-XM_016017502.2	regulation of mitotic cell cycle	
	FLD21.2.1	LOC107410242	rna-XM_025070976.1	anatomical structure morphogenesis; tissue development; regulation of gene expression; cellular process; developmental process; regulation of cellular process
	LOC107409704	rna-XM_016017140.2	Cell wall	
	LOC107409426	rna-XM_016016863.2	Zinc finger protein	
LOC107410070	rna-XM_016017488.1	regulation of mitotic cell cycle		
LOC107409919	rna-XM_016017343.2	LRR receptor-like serine/threonine-protein At3g47570		
LOC107409987	rna-XM_016017405.2	NAC domain-containing protein		
LOC107410070	rna-XM_025070727.1	regulation of mitotic cell cycle		
LOC107410143	rna-XM_016017558.2	Leucine-rich repeat-containing protein		
LOC107409642	rna-XM_016017070.2	regulation of cellular process		
94.450–96.259	FW21.2.2	LOC107409953	rna-XM_016017375.2	LRR receptor-like serine/threonine-protein At3g47570
		LOC107409987	rna-XM_016017405.2	NAC domain-containing protein
	LOC112490770	rna-XM_025071274.1	LRR receptor-like serine/threonine-protein EFR	
	LOC107409919	rna-XM_016017343.2	LRR receptor-like serine/threonine-protein At3g47570	
	LOC107409426	rna-XM_016016863.2	Zinc finger protein	
	LOC107410143	rna-XM_016017551.2	Leucine-rich repeat-containing protein	
	LOC107409998	rna-XM_016017417.2	LRR receptor-like serine/threonine-protein EFR	
	LOC107410143	rna-XM_016017558.2	Leucine-rich repeat-containing protein	
	LOC107409426	rna-XM_016016863.2	Zinc finger protein	
	FTD21.2.2	LOC107410143	rna-XM_016017551.2	Leucine-rich repeat-containing protein
LOC107409953	rna-XM_016017375.2	LRR receptor-like serine/threonine-protein At3g47570		
LOC107410143	rna-XM_016017558.2	Leucine-rich repeat-containing protein		
LOC107409704	rna-XM_016017148.2	Cell wall		
LOC107409953	rna-XM_016017375.2	LRR receptor-like serine/threonine-protein At3g47570		
FLD21.2.1	LOC112490770	rna-XM_025071274.1	LRR receptor-like serine/threonine-protein EFR	
	LOC107410143	rna-XM_016017551.2	Leucine-rich repeat-containing protein	
	LOC107410070	rna-XM_016017481.1	regulation of mitotic cell cycle	
	LOC107409704	rna-XM_016017134.2	Cell wall	

Table 9. Cont.

Range (cM)	QTL Name	Candidate Genes	Candidate Gene ID	Gene Annotation
		LOC107409998	rna-XM_016017417.2	LRR receptor-like serine/threonine-protein EFR
		LOC107410070	rna-XM_025070726.1	regulation of mitotic cell cycle
		LOC107410070	rna-XM_016017502.2	regulation of mitotic cell cycle
		LOC107410242	rna-XM_025070976.1	anatomical structure morphogenesis; tissue development; regulation of gene expression; cellular process; developmental process; regulation of cellular process
		LOC107409704	rna-XM_016017140.2	Cell wall
		LOC107409426	rna-XM_016016863.2	Zinc finger protein
		LOC107410070	rna-XM_016017488.1	regulation of mitotic cell cycle
		LOC107409919	rna-XM_016017343.2	LRR receptor-like serine/threonine-protein At3g47570
		LOC107409987	rna-XM_016017405.2	NAC domain-containing protein
		LOC107410070	rna-XM_025070727.1	regulation of mitotic cell cycle
		LOC107410143	rna-XM_016017558.2	Leucine-rich repeat-containing protein
		LOC107409642	rna-XM_016017070.2	regulation of cellular process
		LOC107431773	rna-XM_016042763.2	E3 ubiquitin-protein ligase
		LOC107431775	rna-XM_025079541.1	Cindole-3-acetic acid amido synthetase activity
		LOC107431773	rna-XM_016042765.2	E3 ubiquitin-protein ligase
		LOC107431773	rna-XM_025066560.1	E3 ubiquitin-protein ligase
28.383	FTD21.12.1	LOC107431775	rna-XM_016042766.2	indole-3-acetic acid amido synthetase activity
		LOC107431773	rna-XM_025066561.1	E3 ubiquitin-protein ligase
		LOC107431772	rna-XM_016042762.2	plant-type secondary cell wall biogenesis
		LOC107431773	rna-XM_016042764.2	E3 ubiquitin-protein ligase
	FW21.12.1	-	-	-
		LOC107409953	rna-XM_016017375.2	LRR receptor-like serine/threonine-protein At3g47570
		LOC112490770	rna-XM_025071274.1	LRR receptor-like serine/threonine-protein EFR
94.450–96.259	FW21.2.2	LOC107409919	rna-XM_016017343.2	LRR receptor-like serine/threonine-protein At3g47570
		LOC107410143	rna-XM_016017551.2	Leucine-rich repeat-containing protein
		LOC107409998	rna-XM_016017417.2	LRR receptor-like serine/threonine-protein EFR
		LOC107410143	rna-XM_016017558.2	Leucine-rich repeat-containing protein
		LOC107409704	rna-XM_016017148.2	Cell wall
		LOC107409953	rna-XM_016017375.2	LRR receptor-like serine/threonine-protein At3g47570
		LOC112490770	rna-XM_025071274.1	LRR receptor-like serine/threonine-protein EFR
		LOC107410143	rna-XM_016017551.2	Leucine-rich repeat-containing protein
		LOC107410070	rna-XM_016017481.1	regulation of mitotic cell cycle
		LOC107409704	rna-XM_016017134.2	Cell wall
		LOC107409998	rna-XM_016017417.2	LRR receptor-like serine/threonine-protein EFR
		LOC107410070	rna-XM_025070726.1	regulation of mitotic cell cycle
91.137–96.259	FLD21.2.1	LOC107410070	rna-XM_016017502.2	regulation of mitotic cell cycle
		LOC107410242	rna-XM_025070976.1	anatomical structure morphogenesis; tissue development; regulation of gene expression; cellular process; developmental process; regulation of cellular process
		LOC107409704	rna-XM_016017140.2	Cell wall
		LOC107409426	rna-XM_016016863.2	Zinc finger protein
		LOC107410070	rna-XM_016017488.1	regulation of mitotic cell cycle
		LOC107409919	rna-XM_016017343.2	LRR receptor-like serine/threonine-protein At3g47570
		LOC107410070	rna-XM_025070727.1	regulation of mitotic cell cycle
		LOC107410143	rna-XM_016017558.2	Leucine-rich repeat-containing protein

Table 9. Cont.

Range (cM)	QTL Name	Candidate Genes	Candidate Gene ID	Gene Annotation		
64.380–86.663	FTD21.8.1	LOC107423900	rna-XM_016033552.2	cell wall; auxin-activated signaling pathway		
		LOC107423928	rna-XM_025076890.1	cytokinin metabolic process		
		LOC107423913	rna-XM_016033565.2	indoleacetic acid biosynthetic process; response to auxin		
		LOC107423813	rna-XM_016033450.2	E3 ubiquitin-protein ligase		
		LOC107423814	rna-XM_016033451.1	cell wall; cell wall modification		
		LOC107423928	rna-XM_025076888.1	cytokinin metabolic process		
		LOC107423861	rna-XM_016033508.2	protein serine/threonine kinase activity		
		LOC107423912	rna-XM_016033564.2	indoleacetic acid biosynthetic process; response to auxin		
		LOC107423811	rna-XM_016033446.2	Transcription factor bHLH		
		LOC107423821	rna-XM_025076730.1	mitotic cell cycle; regulation of cell cycle		
		LOC107423857	rna-XM_016033503.2	cell wall		
		LOC107423801	rna-XM_016033440.1	E3 ubiquitin-protein ligase		
		LOC107423922	rna-XM_016033576.2	plant-type cell wall biogenesis; regulation of meristem growth		
		LOC107423928	rna-XM_016033582.2	cytokinin metabolic process		
		LOC107423848	rna-XM_016033491.2	cell wall; Pectin methyltransferase		
		LOC107423928	rna-XM_025076887.1	cytokinin metabolic process		
		LOC107423928	rna-XM_025076889.1	cytokinin metabolic process		
		LOC107423846	rna-XM_016033490.2	cell wall; pectinesterase activity; cell wall modification; pectin catabolic process		
		LOC107423858	rna-XM_025076143.1	cell wall		
		LOC107423925	rna-XM_016033579.2	cell wall		
		LOC107423923	rna-XM_016033577.2	protein serine/threonine kinase activity		
		LOC107423815	rna-XM_025076224.1	putative pectinesterase/pectinesterase inhibitor 45-like		
		LOC107423897	rna-XM_016033547.2	Leucine-rich repeat receptor-like protein kinase		
		LOC107423905	rna-XM_016033556.2	response to auxin		
		LOC107423856	rna-XM_025076290.1	cell wall		
		LOC107423846	rna-XM_016033489.2	cell wall; Pectinesterase PPE8B		
		LOC107423903	rna-XM_016033555.1	cell wall		
		LOC107423821	rna-XM_016033457.2	mitotic cell cycle; meiotic cell cycle; regulation of cell cycle		
		LOC107423816	rna-XM_016033453.2	E3 ubiquitin-protein ligase		
		LOC107423881	rna-XM_016033528.2	Cell wall		
		LOC107423820	rna-XM_016033456.2	Pectinesterase 54		
		21.382	FTD20.11.1	-	-	-
			FW20.11.1	-	-	-

4. Discussion

4.1. Advantages of Constructing a High-Density Genetic Linkage Map Based on Bin Markers

In this study, the genomes of “JMS2” and “Xing16” and their F_1 progeny (165 in number) were resequenced. The average coverage depth of the parental genomes was $>20\times$ with an average genome coverage $>90\%$, while the average coverage depth of the offspring was $4.14\times$ with an average genome coverage $>76.33\%$. A total of 2398 recombination bin markers comprising 116,312 SNP markers were mapped onto 12 LGs. The total length of the linkage map was 1074.33 cM with an average bin intermarker distance of 0.45 cM. The map presented in this study identified manifold SNP markers (116,312) in comparison to those in the six genetic linkage maps already available (2540–8158) with the highest sequencing depth. In addition, the genetic map presented used a bin-marker-based mapping to classify consecutive SNP markers that did not undergo recombination as bins, thus avoiding the probability of errors occurring in the SNP calculation due to the detection of numerous loci and collection of a large amount of data. Bin markers have been used to develop high-density genetic maps in many crops, such as radish [39], brassica napus [40], and melon [41],

but not so much on fruit trees, such as hawthorn [42], pear [18], and grapes [26,43]. Our study found the highest number of SNP markers that had shorter intermarker gaps, were of high quality, and demonstrated enhanced precision in jujube. This will be more conducive to determining the location of trait candidate gene segments.

4.2. Mapping of QTLs Associated with Traits Relating to Fruit Size in Jujube

The identification of QTLs affecting fruit size traits in jujube has been less studied when compared to other fruit tree species. In this study, 15 QTLs associated with fruit size traits were mapped, and candidate QTLs that were identified through molecular analyses in at least two years of a three-year study, related to at least two of the three indicators of fruit size (SFW, FLD, and FTD), or had an LOD threshold ≥ 3.5 and a PVE $\geq 10\%$ in any one year were selected for gene mining. A total of 113 genes were identified to be located on LG2, 8, and 12. Previous studies have also mapped QTLs related to jujube fruit size, but the results were inconsistent [44,45]. This may be due to differences in groups, environment, and other aspects. Although the location of the QTL varies greatly, we can analyze the function of these 113 genes in other species and may find some candidate genes related to fruit development, laying the foundation for jujube breeding (Table 9).

4.3. In Silico Prediction of the Putative Functions of the Candidate Genes Determining Fruit Size

Rapid cell division, cell elongation, and duration of the cell cycle determine the final size, shape, and weight of the fruit. The family of serine/threonine protein kinases and cell cycle proteins together with phosphorylated compounds act at two checkpoints to initiate DNA replication and mitosis to regulate the cell cycle [46]. During the growth and development of pear fruits, pectin esterase is associated with the relaxation and extension of the cell wall pulp, which may lead to an increase in the number of cells. Similarly, cellulase facilitates cell division when required while regulating their growth and development [47]. Cell wall biogenesis also plays an important role in cell expansion and unidirectional elongation [48]. A homolog of an *Arabidopsis* ubiquitin-specific protease, *ZjDA3*, was found to be a negative regulator of fruit size in jujube [49]. In addition, the MYB TFs are also known to demonstrate regulatory effects on fruit development. The *R2R3-MYB* TF was found to alter the size and shape of cells in the fruits and leaves of tomatoes [50].

Plant hormones directly regulate the fruit size and shape growth and development by altering the expression of early response genes in horticultural plants. The high auxin content depressed the expression of *MdAux/IAA2*, and the downregulated expression of *MdAux/IAA2* led to the formation of a large fruit size apple [22]. An important role for auxin in the regulation of fruit development, especially at the fruit enlargement stage, and three single nucleotide polymorphism (SNP) markers were also closely associated with fruit weight in loquat [20]. Studies on the direct regulation of fruit size and shape by hormones are more common in tomato and cucumber. ABA participates in the CsTRM5-mediated cell expansion during fruit elongation [51], and the auxin-responsive protein CsARP1 promotes cell expansion and fruit elongation in cucumber [23]. In a study of strawberry fruit shape, different expression genes were mainly enriched in DNA replication, cell cycle, plant hormone synthesis, and signal transduction, including auxin-related genes in elongated strawberry fruit [52]. Six candidate genes for fruit size were found to be involved in the regulation of the cell cycle and hormone biosynthesis pathways, including *LOC107404981* and *LOC107406728*, which may be involved in the molecular regulation of fruit size in jujube [53]. These studies have shown that fruit size and shape are inseparable from plant hormones and can provide certain reference value for further research. In this study, we identified 113 candidate genes regulating fruit size in jujube. These genes were determined to be involved in the regulation of cell division, cell cycle, and cell wall metabolism; biosynthesis of phytohormones (ABA, IAA, and auxin); and encoding of enzymes, transcription factors, and ZFPs.

In conclusion, we carried out high-density genetic bin mapping for the identification of reliable QTLs and candidate genes in a single F_1 hybrid population in jujube. These results provide a foundation for further research on fruit size in jujube and also provide a theoretical basis for molecular breeding of new jujube varieties.

Author Contributions: C.W. and M.L. conceived and designed the experiments. F.Y. provided support with experimental materials. Q.Q., T.G., Z.W. and J.W. analyzed the data. T.G., J.B., Z.Y. and Y.X. were involved in the experiment and provided technical and theoretical support for this work. Q.Q. and T.G. wrote the paper. C.W. and M.L. revised the intellectual content of this paper. All authors have read and agreed to the published version of the manuscript.

Funding: This research was supported by the Major Scientific and Technological Projects of Xinjiang Production and Construction Corps (2017DB006), Innovation and Entrepreneurship Platform and Base Construction Project of Xinjiang Production and Construction Corps (2019CB001), and earmarked fund of Xinjiang Jujube Industrial Technology System (XJCYTX-01). We wish to express our thanks for their financial support.

Data Availability Statement: The data presented in the study are deposited in the NCBI repository, accession number is PRJNA996341 (<https://www.ncbi.nlm.nih.gov/sra/PRJNA996341>).

Acknowledgments: The fruit of jujube cultivars “JMS2” × “Xing16” and their F_1 segregating population consisting of 165 progenies were obtained from Hebei Agricultural University, Hebei, China.

Conflicts of Interest: The authors declare no competing interest.

References

- Liu, M.; Wang, J.; Wang, L.; Liu, P.; Zhao, J.; Zhao, Z.; Yao, S.; Stănică, F.; Liu, Z.; Wang, L. The historical and current research progress on jujube—A superfruit for the future. *Hortic. Res.* **2020**, *7*, 119. [[CrossRef](#)] [[PubMed](#)]
- Liu, M.; Wang, J. Fruit scientific research in New China in the past 70 years: Chinese jujube. *J. Fruit Sci.* **2019**, *36*, 1369–1381.
- Meng-jun, L.; Jiu-rui, W.; Ping, L.; Jin, Z.; Zhi-hui, Z.; Li, D.; Xian-Song, L.; Zhi-guo, L. Historical achievements and frontier advances in the production and research of Chinese jujube (*Ziziphus jujuba*) in China. *Acta Hort. Sin.* **2015**, *42*, 1683.
- Richardson, J.E.; Fay, M.F.; Cronk, Q.C.; Bowman, D.; Chase, M.W. A phylogenetic analysis of Rhamnaceae using rbcL and trnL-F plastid DNA sequences. *Am. J. Bot.* **2000**, *87*, 1309–1324. [[CrossRef](#)]
- Qu, Z.-Z.; Wang, Y.-H. *Chinese Fruit Trees Record—Chinese Jujube*; The Forestry Publishing House of China: Beijing, China, 1993.
- Liu, M.J.; Wang, M. *Germplasm Resources of Chinese Jujube*; China Forestry Publishing House: Beijing, China, 2009.
- Yang, H.; Zou, Y.; Li, X.; Zhang, M.; Zhu, Z.; Xu, R.; Xu, J.; Deng, X.; Cheng, Y. QTL analysis reveals the effect of CER1-1 and CER1-3 to reduce fruit water loss by increasing cuticular wax alkanes in citrus fruit. *Postharvest Biol. Technol.* **2022**, *185*, 111771. [[CrossRef](#)]
- Calle, A.; Wünsch, A. Multiple-population QTL mapping of maturity and fruit-quality traits reveals LG4 region as a breeding target in sweet cherry (*Prunus avium* L.). *Hortic. Res.* **2020**, *7*, 127. [[CrossRef](#)]
- Wu, Y.; Popovsky-Sarid, S.; Tikunov, Y.; Borovsky, Y.; Baruch, K.; Visser, R.G.; Paran, I.; Bovy, A. *CaMYB12-like* underlies a major QTL for flavonoid content in pepper (*Capsicum annuum*) fruit. *New Phytol.* **2023**, *237*, 2255–2267. [[CrossRef](#)] [[PubMed](#)]
- Lu, J.Y. *Study on Identification of Hybrids and Hereditary Variation of Natural Pollinated Chinese Jujube Seedlings*; Agricultural University of Hebei: Baoding, China, 2003.
- Xu, L.S. QTL Mapping of Fruit Traits and Superior Genotypes Selecting in Chinese Jujube (*Ziziphus jujuba* Mill.). Ph.D. Thesis, Agricultural University of Hebei, Baoding, China, 2012.
- Qi, J.; Dong, Z.; Mao, Y.M.; Shen, L.Y.; Zhang, Y.X.; Liu, J.; Wang, X.L. Construction of a Dense Genetic Linkage Map and QTL Analysis of Trunk Diameter in Chinese Jujube. *Sci. Silvar Sin.* **2009**, *45*, 44–49.
- Shen, L.Y. Construction of Genetic Linkage Map and Mapping QTLs for Some Traits in Chinese Jujube (*Ziziphus jujuba* Mill.). Ph.D. Thesis, Agricultural University of Hebei, Baoding, China, 2005.
- Liu, M.-J.; Zhao, J.; Cai, Q.-L.; Liu, G.-C.; Wang, J.-R.; Zhao, Z.-H.; Liu, P.; Dai, L.; Yan, G.; Wang, W.-J. The complex jujube genome provides insights into fruit tree biology. *Nat. Commun.* **2014**, *5*, 5315. [[CrossRef](#)] [[PubMed](#)]
- Yan, F.; Luo, Y.; Bao, J.; Pan, Y.; Wang, J.; Wu, C.; Liu, M. Construction of a highly saturated genetic map and identification of quantitative trait loci for leaf traits in jujube. *Front. Plant Sci.* **2022**, *13*, 1001850. [[CrossRef](#)]
- Zhang, Z.; Wei, T.; Zhong, Y.; Li, X.; Huang, J. Construction of a high-density genetic map of *Ziziphus jujuba* Mill. using genotyping by sequencing technology. *Tree Genet. Genomes* **2016**, *12*, 76. [[CrossRef](#)]
- Hou, L.; Chen, W.; Zhang, Z.; Pang, X.; Li, Y. Genome-wide association studies of fruit quality traits in jujube germplasm collections using genotyping-by-sequencing. *Plant Genome* **2020**, *13*, e20036. [[CrossRef](#)] [[PubMed](#)]

18. Qin, M.-F.; Li, L.-T.; Singh, J.; Sun, M.-Y.; Bai, B.; Li, S.-W.; Ni, J.-P.; Zhang, J.-Y.; Zhang, X.; Wei, W.-L. Construction of a high-density bin-map and identification of fruit quality-related quantitative trait loci and functional genes in pear. *Hortic. Res.* **2022**, *9*, uhac141. [[CrossRef](#)] [[PubMed](#)]
19. Vision, T.J.; Brown, D.G.; Shmoys, D.B.; Durrett, R.T.; Tanksley, S.D. Selective mapping: A strategy for optimizing the construction of high-density linkage maps. *Genetics* **2000**, *155*, 407–420. [[CrossRef](#)]
20. Peng, Z.; Zhao, C.; Li, S.; Guo, Y.; Xu, H.; Hu, G.; Liu, Z.; Chen, X.; Chen, J.; Lin, S.; et al. Integration of genomics, transcriptomics and metabolomics identifies candidate loci underlying fruit weight in loquat. *Hortic. Res.* **2022**, *9*, uhac037. [[CrossRef](#)] [[PubMed](#)]
21. Wang, Y.; Aizezi, S.; Li, Y.L.; Sun, F.; Wu, G.H. Inheritance trend of the fruit traits of ‘huozhouheiyu’ grape. *Acta Bot. Boreal-Occident. Sin.* **2015**, *35*, 275–281.
22. Bu, H.; Sun, X.; Yue, P.; Qiao, J.; Sun, J.; Wang, A.; Yuan, H.; Yu, W. The MdAux/IAA2 Transcription Repressor Regulates Cell and Fruit Size in Apple Fruit. *Int. J. Mol. Sci.* **2022**, *23*, 9454. [[CrossRef](#)]
23. Che, G.; Song, W.; Zhang, X. Gene network associates with CsCRC regulating fruit elongation in cucumber. *Veg. Res.* **2023**, *3*, 7. [[CrossRef](#)]
24. Ma, B.; Zhao, S.; Wu, B.; Wang, D.; Peng, Q.; Owiti, A.; Fang, T.; Liao, L.; Ogutu, C.; Korban, S.S.; et al. Construction of a high density linkage map and its application in the identification of QTLs for soluble sugar and organic acid components in apple. *Tree Genet. Genomes* **2015**, *12*, 1. [[CrossRef](#)]
25. Wang, L.; Li, X.; Wang, L.; Xue, H.; Wu, J.; Yin, H.; Zhang, S. Construction of a high-density genetic linkage map in pear (*Pyrus communis* × *Pyrus pyrifolia nakai*) using SSRs and SNPs developed by SLAF-seq. *Sci. Hort.* **2017**, *218*, 198–204. [[CrossRef](#)]
26. Jiang, J.; Fan, X.; Zhang, Y.; Tang, X.; Li, X.; Liu, C.; Zhang, Z. Construction of a High-Density Genetic Map and Mapping of Firmness in Grapes (*Vitis vinifera* L.) Based on Whole-Genome Resequencing. *Int. J. Mol. Sci.* **2020**, *21*, 797. [[CrossRef](#)] [[PubMed](#)]
27. Zhang, Q.; Liu, J.; Liu, W.; Liu, N.; Zhang, Y.; Xu, M.; Liu, S.; Ma, X.; Zhang, Y. Construction of a High-Density Genetic Map and Identification of Quantitative Trait Loci Linked to Fruit Quality Traits in Apricots Using Specific-Locus Amplified Fragment Sequencing. *Front Plant Sci* **2022**, *13*, 798700. [[CrossRef](#)] [[PubMed](#)]
28. Paterson, A.H.; Brubaker, C.L.; Wendel, J.F. A rapid method for extraction of cotton (*Gossypium* spp.) genomic DNA suitable for RFLP or PCR analysis. *Plant Mol. Biol. Report.* **1993**, *11*, 122–127. [[CrossRef](#)]
29. Bolger, A.M.; Lohse, M.; Usadel, B. Trimmomatic: A flexible trimmer for Illumina sequence data. *Bioinformatics* **2014**, *30*, 2114–2120. [[CrossRef](#)]
30. Li, H.; Durbin, R. Fast and accurate short read alignment with Burrows–Wheeler transform. *Bioinformatics* **2009**, *25*, 1754–1760. [[CrossRef](#)]
31. McKenna, A.; Hanna, M.; Banks, E.; Sivachenko, A.; Cibulskis, K.; Kernysky, A.; Garimella, K.; Altshuler, D.; Gabriel, S.; Daly, M. The Genome Analysis Toolkit: A MapReduce framework for analyzing next-generation DNA sequencing data. *Genome Res.* **2010**, *20*, 1297–1303. [[CrossRef](#)]
32. Cingolani, P.; Platts, A.; Wang, L.L.; Coon, M.; Nguyen, T.; Wang, L.; Land, S.J.; Lu, X.; Ruden, D.M. A program for annotating and predicting the effects of single nucleotide polymorphisms, SnpEff: SNPs in the genome of *Drosophila melanogaster* strain w¹¹¹⁸; iso-2; iso-3. *fly* **2012**, *6*, 80–92. [[CrossRef](#)]
33. Liu, D.; Ma, C.; Hong, W.; Huang, L.; Liu, M.; Liu, H.; Zeng, H.; Deng, D.; Xin, H.; Song, J. Construction and analysis of high-density linkage map using high-throughput sequencing data. *PLoS ONE* **2014**, *9*, e98855. [[CrossRef](#)]
34. Yandell, B.S.; Mehta, T.; Banerjee, S.; Shriner, D.; Venkataraman, R.; Moon, J.Y.; Neely, W.W.; Wu, H.; Von Smith, R.; Yi, N. R/qtlbim: QTL with Bayesian interval mapping in experimental crosses. *Bioinformatics* **2007**, *23*, 641–643. [[CrossRef](#)]
35. Zhao, J.; Xu, Y.; Li, H.; Yin, Y.; An, W.; Li, Y.; Wang, Y.; Fan, Y.; Wan, R.; Guo, X. A SNP-based high-density genetic map of leaf and fruit related quantitative trait loci in wolfberry (*Lycium* Linn.). *Front. Plant Sci.* **2019**, *10*, 977. [[CrossRef](#)]
36. Pereira, L.; Ruggieri, V.; Pérez, S.; Alexiou, K.G.; Fernández, M.; Jahrmann, T.; Pujol, M.; Garcia-Mas, J. QTL mapping of melon fruit quality traits using a high-density GBS-based genetic map. *BMC Plant Biol.* **2018**, *18*, 324. [[CrossRef](#)] [[PubMed](#)]
37. Huang, X.; Feng, Q.; Qian, Q.; Zhao, Q.; Wang, L.; Wang, A.; Guan, J.; Fan, D.; Weng, Q.; Huang, T. High-throughput genotyping by whole-genome resequencing. *Genome Res.* **2009**, *19*, 1068–1076. [[CrossRef](#)] [[PubMed](#)]
38. Tatusov, R.L.; Koonin, E.V.; Lipman, D.J. A Genomic Perspective on Protein Families. *Science* **1997**, *278*, 631–637. [[CrossRef](#)] [[PubMed](#)]
39. Luo, X.; Xu, L.; Wang, Y.; Dong, J.; Chen, Y.; Tang, M.; Fan, L.; Zhu, Y.; Liu, L. An ultra-high-density genetic map provides insights into genome synteny, recombination landscape and taproot skin colour in radish (*Raphanus sativus* L.). *Plant Biotechnol. J.* **2020**, *18*, 274–286. [[CrossRef](#)] [[PubMed](#)]
40. Dong, Z.; Alam, M.K.; Xie, M.; Yang, L.; Liu, J.; Helal, M.; Huang, J.; Cheng, X.; Liu, Y.; Tong, C. Mapping of a major QTL controlling plant height using a high-density genetic map and QTL-seq methods based on whole-genome resequencing in *Brassica napus*. *G3* **2021**, *11*, jkab118. [[CrossRef](#)] [[PubMed](#)]
41. Lian, Q.; Fu, Q.; Xu, Y.; Hu, Z.; Zheng, J.; Zhang, A.; He, Y.; Wang, C.; Xu, C.; Chen, B. QTLs and candidate genes analyses for fruit size under domestication and differentiation in melon (*Cucumis melo* L.) based on high resolution maps. *BMC Plant Biol.* **2021**, *21*, 126. [[CrossRef](#)]
42. Zhao, Y.; Zhao, Y.; Guo, Y.; Su, K.; Shi, X.; Liu, D.; Zhang, J. High-density genetic linkage-map construction of hawthorn and QTL mapping for important fruit traits. *PLoS ONE* **2020**, *15*, e0229020. [[CrossRef](#)]

43. Shi, G.; Sun, D.; Wang, Z.; Liu, X.; Guo, J.; Zhang, S.; Zhao, Y.; Ai, J. Construction of a resequencing-based high-density genetic map for grape using an interspecific population (*Vitis amurensis* × *Vitis vinifera*). *Hortic. Environ. Biotechnol.* **2022**, *63*, 489–497. [[CrossRef](#)]
44. Bao, J.K. Construction of High-Density Genetic Map and QTL Mapping of Fruit Size and Sugar-Acid Traits on 'JMS2' × 'Jiaocheng 5' Jujuba Hybrid Progeny. Master's Thesis, Tarim University, Alar, China, 2022.
45. Wang, Z. High-density Genetic Map Construction and QTL Mapping of Agronomic Traits of *Ziziphus jujuba* Mill. Ph.D. Thesis, College of Forestry Northwest A&F University, Yangling, China, 2020.
46. Zhang, H.; Tan, J.; Zhang, M.; Huang, S.; Chen, X. Comparative transcriptomic analysis of two bottle gourd accessions differing in fruit size. *Genes* **2020**, *11*, 359. [[CrossRef](#)]
47. Liu, X. Studies on Mechanism of Fruit Growth and Development of Different Ripening-Season of Pears. Ph.D. Thesis, Sichuan Agriculture University, Ya'an, China, 2008.
48. Bashline, L.; Lei, L.; Li, S.; Gu, Y. Cell wall, cytoskeleton, and cell expansion in higher plants. *Mol. Plant* **2014**, *7*, 586–600. [[CrossRef](#)]
49. Guo, M.; Zhang, Z.; Cheng, Y.; Li, S.; Shao, P.; Yu, Q.; Wang, J.; Xu, G.; Zhang, X.; Liu, J. Comparative population genomics dissects the genetic basis of seven domestication traits in jujube. *Hortic. Res.* **2020**, *7*, 89. [[CrossRef](#)] [[PubMed](#)]
50. Mahjoub, A.; Hernould, M.; Joubès, J.; Decendit, A.; Mars, M.; Barriou, F.; Hamdi, S.; Delrot, S. Overexpression of a grapevine R2R3-MYB factor in tomato affects vegetative development, flower morphology and flavonoid and terpenoid metabolism. *Plant Physiol. Biochem.* **2009**, *47*, 551–561. [[CrossRef](#)] [[PubMed](#)]
51. Xie, Y.; Liu, X.; Sun, C.; Song, X.; Li, X.; Cui, H.; Guo, J.; Liu, L.; Ying, A.; Zhang, Z.; et al. CsTRM5 regulates fruit shape via mediating cell division direction and cell expansion in cucumber. *Hortic. Res.* **2023**, *10*, uhad007. [[CrossRef](#)] [[PubMed](#)]
52. Li, Z.; Song, X.; Li, H.; Zhang, Z.; Zhang, J. Transcriptome and hormones analysis provide insights into elongated fruit somaclonal mutant in 'Akihime' strawberry. *Sci. Hortic.* **2023**, *309*, 111608. [[CrossRef](#)]
53. Yang, L.; Zhou, H.i.; Bo, W.h.; Li, Y.y.; Pang, X.m. Identification of genes related with jujube fruit size based on selective sweep analysis. *J. Beijing For. Univ.* **2019**, *41*, 30–36.

Disclaimer/Publisher's Note: The statements, opinions and data contained in all publications are solely those of the individual author(s) and contributor(s) and not of MDPI and/or the editor(s). MDPI and/or the editor(s) disclaim responsibility for any injury to people or property resulting from any ideas, methods, instructions or products referred to in the content.